Acoustic Emission of Bubbly Flow and Its Size Distribution Spectrum

Li Chen (1), Shane Wood (2), Stephen Moore (1) and Binh Nguyen (2)

(1) Maritime Platforms Division, DSTO, Melbourne, Australia
(2) Maritime Operations Division, DSTO, Edinburgh, Australia

ABSTRACT

Acoustic emissions were used to predict bubble size distribution resulting from air discharged through a single orifice. Air was discharged at a particular flow rate through an orifice into quiescent water contained in a large tank. Acoustic measurements were made at different locations in the tank using a single hydrophone and the experiments were carried out with two orifice sizes. The bubble size distribution was estimated based on the acoustic measurement. It was found that the model used to estimate the bubble size distribution was sensitive to the initial displacement of bubbles. The model predicted that an increased number of large bubbles were produced by a high flow rate through a large orifice compared with a low flow rate through a small orifice. This result was verified qualitatively in the experiments. Further work will be carried out to improve the measurement of acoustic emissions and to quantify the bubble generation rate in the experiments.

INTRODUCTION

Noise generated by bubbles is a complex phenomenon and has attracted intensive research for many years because of its importance to a range of applications, such as its contribution to ocean background noise, its use in medical diagnostic techniques and its significance to the stealth of naval platforms. A comprehensive coverage of this topic can be found in Leighton (1994). Examples of previous studies in this field include works by Strasberg (1956), Leighton & Walton (1987), Longuet-Higgins (1990) and Deane & Stokes (2008). These studies have focused on a single bubble, or bubble formation at a low flow rate. The frequency of acoustic waves generated by the formation of a bubble at an orifice at low gas flow rates can be theoretically calculated and has been used to size bubbles. However, at higher flow rates, multiple bubbles are involved, and there is no simple theory that can be used to predict the corresponding acoustic field due to different mechanisms involved in the bubble formation (Leighton 1994, Blake 1986, and Gavigan et al. 1974). For example, the sound emission due to bubble fragmentation caused by turbulence may be different to that of a bubble excited by its detachment from an orifice. At a high air flow rate, the formation and interaction of bubbles are affected by orifice size and induced liquid flow. This is particularly true for cases with the most practical relevance. For these reasons, many experimental and theoretic studies have been reported to address these issues (Gavigan 1974, Leighton 1994, Chen & Li 1998, Chen et al. 1999, Chen et al. 2001, and Deane & Stokes 2008). However, more research is required to better understand the mechanism of noise generation in a bubbly flow.

The aim of this study was to model the relationship between the acoustic emission and the bubble generation rate of a bubbly plume. The effect of air flow rate and orifice size on acoustic emission was investigated though experimentation. The bubble generation rate and air flow rate was then esti-mated from the measured acoustic emission, based on a model developed by Leighton and White (2011).

THEORY

As discussed above, many studies have used acoustic measurements to estimate the size of bubbles that form at very low flow rates, or to estimate the size of bubbles in bubbly plumes with a limited range of bubble sizes. Such applications do not necessarily require information on the magnitude of sound pressure induced by bubble oscillation, but require the frequency of acoustic waves emitted by the bubbles. Modelling the relationship between acoustic emission and bubble generation rate for high flow rates is more challenging because of the range of bubble sizes and interaction of bubbles in the plume. In addition, estimating the size distribution of bubbles in a bubbly flow requires an accurate measurement of the sound pressure. Leighton & White (2011) provided a model to calculate the acoustic pressure radiated by a single bubble pulsating at resonance frequency ω_0 at time t and a distance r (far field)

$$P_b(t) \approx \mathrm{Re}\left\{ \rho_0 \frac{(\omega_0 R_0)^2}{r} R_{\varepsilon 0i} e^{j\omega_0(t-t_i)} e^{-\omega_0 \delta_{tot}(t-t_i)/2} \mathrm{H}(t-t_i) \right\}, \quad (1)$$

R_0 is the initial bubble size, $R_{\varepsilon 0i}$ is the initial displacement of the bubble's wall, ρ_0 is the density in the far field, H is the Heaviside step function, and t_i is retard time. The decay of the pressure induced by the oscillating bubble is determined by the dimensionless damping constant δ_{tot} defined by Leighton (1998) as

$$\delta_{tot} = \delta_{th} + \delta_{vis} + \delta_{rad}. \quad (2)$$

The thermal damping constant δ_{th}, the viscous damping constant δ_{vis} and the radiation damping constant δ_{rad} are given by

$$\delta_{th} = 4.41 \times 10^{-4} \sqrt{\omega_0 / 2\pi} \; ;$$

$$\delta_{vic} = \frac{4\mu}{\rho_0 \omega_0 R_0^2} \; ; \qquad (3)$$

$$\delta_{vis} = \frac{\omega_0 R_0}{c} \; .$$

Here μ is viscosity of water and c is speed of sound in the far field. The squared magnitude of the Fourier transform of equation (1) yields

$$|P_{b1}(\omega, R_0)|^2 = \left[\omega_0^2 R_0^3 \frac{\rho_0}{\pi r} \frac{R_{\varepsilon 0 i}}{R_0} \right]^2 \times$$
$$\left(\frac{4\left[(\omega_0 \delta_{tot})^2 + 4\omega^2 \right]}{\left[(\omega_0 \delta_{tot})^2 + 4(\omega_0 - \omega)^2 \right] \left[(\omega_0 \delta_{tot})^2 + 4(\omega_0 + \omega)^2 \right]} \right) . \qquad (4)$$

Considering a bubbly plume and assuming the oscillation of each bubble is not correlated to the motion of surrounding bubbles, the monopole emissions of individual bubbles are uncorrelated. If the bubble generation distribution $D(R_0)$ of the bubbly plume is specified, for example using the results from a computational fluid dynamics (CFD) simulation, the power spectral density $S(\omega)$ of far field sound can be calculated by using

$$S(\omega) = \int_0^\infty D(R_0) |P_{01}(\omega, R_0)|^2 dR_0 \qquad (5)$$

The relationship between the initial bubble size R_0 and the resonance is given by (Minnaert 1933)

$$\omega_0 = \frac{1}{R_0} \sqrt{\frac{3\gamma P_0}{\rho}} \; , \qquad (6)$$

in which P_0 is the static pressure and γ is the ratio of specific heats. To solve the model given by equations (4), (5), and (6), the ratio of the initial displacement of a bubble to the initial radius $R_{0\varepsilon i}/R_0$, has to be specified. This parameter is difficult to model because it essentially depends on the bubble formation mechanism, for example fragmentation or coalescence. The specification of $R_{0\varepsilon i}/R_0$ it will be discussed further in the next section.

To estimate the bubble generation rate using the measured acoustic emission, a bubble number spectrum or bubble generation rate spectrum is defined as

$$\psi(n) = \int_{R_{l,n}}^{R_{u,n}} D(R_0) dR_0 \; . \qquad (7)$$

Using this definition, Eq. (5) is approximated as

$$S(\omega_k) \approx \sum_{n=1}^{N_b} \psi(n) |P_{01}(\omega_k, R_n^c)|^2 \; . \qquad (8)$$

If the multiple bubbles are divided into N_b groups, the bubble number spectrum $\psi(n)$ is a single column vector of N_k elements. Eq. 8 forms a $(N_k \times N_b)$ spectral matrix, which will be square if the number of frequencies N_k is equal to the number of bubble groups N_b. In such a case, Eq. (8) can be

solved by inverting the spectrum matrix to obtain the bubble number spectrum as a function of the initial bubble size R_0 and the power spectral density of the sound field. The total flow rate of the system is obtained by integrating the bubble number spectrum.

In this paper, the bubble generation rates were estimated by using the measured acoustic emission. The effect of the parameter $R_{0\varepsilon i}/R_0$ on bubble generation rate was studied and the estimated total flow rates were compared with the measured value.

EXPERIMENTAL APPARATUS

Experiments were carried out in a tank with dimensions 9m×6m×4m ($X \times Y \times D$). Regulated and filtered air was released into the tank through an orifice. The air flow rate was measured with a flow meter and held constant for each experiment. Acoustic measurements were taken at a number of precisely controlled positions specified by the depth d and horizontal distance y from the axis of the orifice. A Brüel & Kjær Type 8103 hydrophone in combination with Brüel & Kjær 2635 charge amplifier was used for acoustic measurements and data was recorded with a Brüel & Kjær PULSE Controller Module 7536 and computer (see Figure 1 for a schematic).
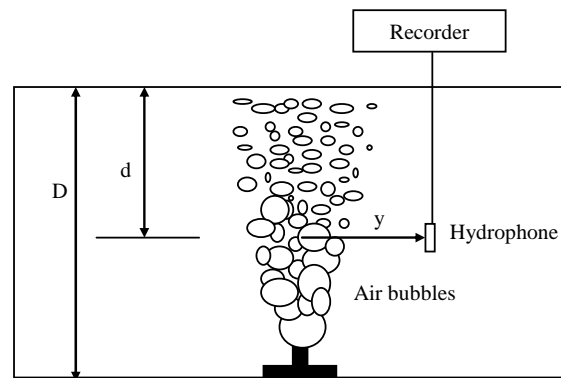

Figure 1. Schematic of the experimental apparatus

Experiments were carried out using two orifice sizes and two airflow rates, as listed in Table 1. For each experiment, 10 seconds of data were recorded with a sampling frequency of 6975.1 Hz. Experiments were repeated with the hydrophone at different positions to investigate the spatial variation of the acoustic emission.

Table 1: Experimental Conditions

Orifice diameter (mm)	Airflow rate (l/s)
2	0.00833
8	0.3333

RESULTS AND DISCUSSION

Acoustic emission

The power spectral density (PSD) of acoustic emissions measured at different horizontal distances from the bubble plume is shown in Figure 2 for the experiment using the 2mm orifice and 0.0083 l/s airflow rate. The background noise level measured during quiescent conditions is also plotted. It can be seen that the noise generated by the bubbles is at least 5 dB higher than the background noise over much of the frequency range of 200 to 1200 Hz for all measurement loca-

tions. Comparing the amplitude of spectra for measurements at distances of 0.5m and 1m suggests the measurement at 0.5m may be in the direct field as indicated by the higher amplitude across the frequency range of 200 – 1200 Hz. Similar amplitudes of measurements at 1m and 2m suggest these measurements may be influenced by the reverberant field.

The preliminary flow visualisation of the bubble plumes was used to determine the size of largest bubbles forming close to the orifice. The minimum frequency of acoustic emissions was calculated to be approximately 500Hz based on the size of the largest bubbles.

The spectrogram of consecutive 0.05 second segments of time record measured at a depth of 2m and 1m from the bubble plume is shown in Figure 3. The high-amplitude component at 250 Hz is due to electrical noise. Other signal components at approximately 500 Hz, 650 Hz, and 920 Hz that are visible in Figure 2 occur intermittently in the spectrogram in Figure 3. This is expected given the transient nature of bubble formation at the orifice. The spectrogram of measurements taken at a depth of 3m and 1m away from the bubble plume is given in Figure 4. Intermittent high amplitude components are present at approximately 750 Hz and 920 Hz. These results demonstrate that the position of the hydrophone affects both the spectral content and amplitude of the measured acoustic emissions. This trend is also demonstrated by comparison of PSD of measurements at depths of 2m and 3m shown in Figure 5. Prominent peaks are present at approximately 750 Hz and 920 Hz for the measurement at 3m depth and only the peak at 920 Hz is seen in the measurement at 2m depth, and the amplitude is approximately 2.5 dB lower.

It is believed that varying bubble size contributes to the variation in spectral content observed for different hydrophone positions, although it is acknowledged that the acoustic response of the tank may not be uniform in the frequency range of interest. Larger bubbles are present close to the orifice and these bubbles subsequently break up as they move up towards the surface interacting with the entrained fluid flow and other bubbles.
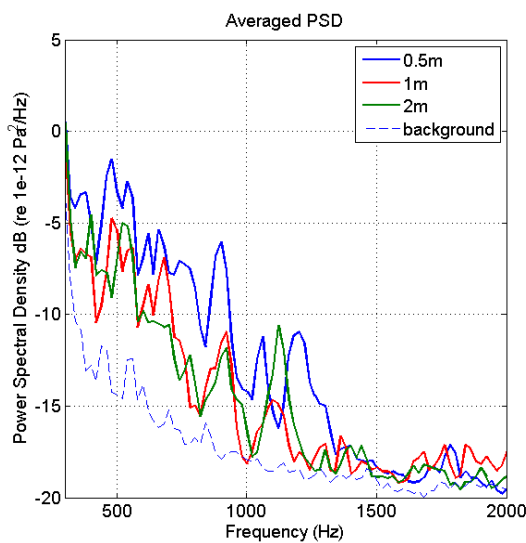

Figure 3. Spectrogram (dB re 10^{-12} Pa^2/Hz) for 2mm orifice measured at d=2m and y=1m

Figure 4. Spectrogram (dB re 10^{-12} Pa^2/Hz) for 2mm orifice measured at d=3m and y=1m

Figure 5. Comparison of PSD of bubble noise measured at different locations for 2mm orifice

Figure 2. PSD of bubble noise for the 2mm orifice measured at d=2m and various horizontal distances away from the centre of the plume.
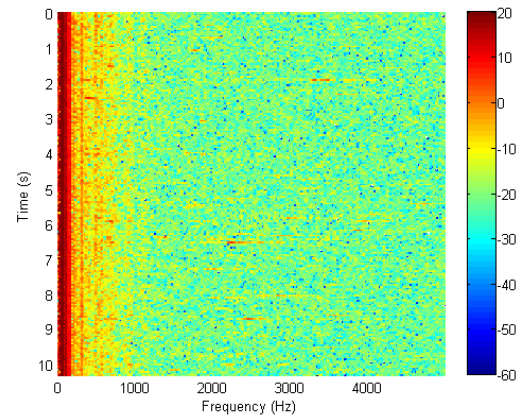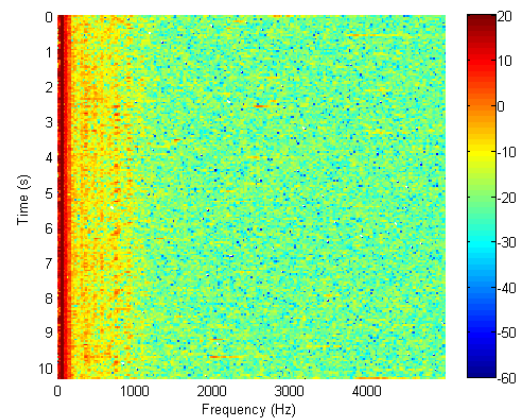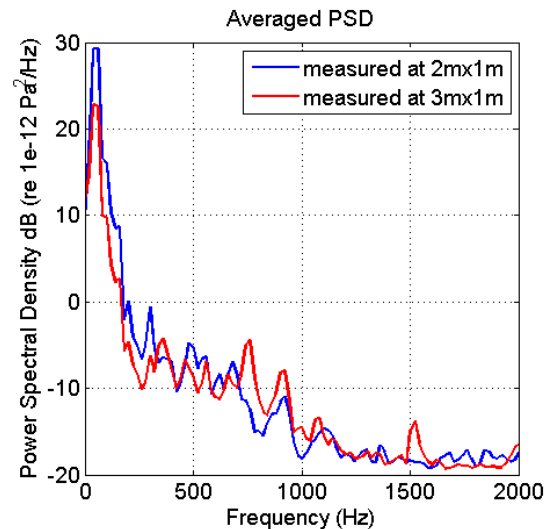
With an increase in the flow rate through the 8mm orifice, the acoustic emission becomes more broadband in nature with an increase in amplitude, particularly in the low frequency region, as shown in Figure 6. This implies the formation of larger bubbles according to Eq. 6, which states that the resonant frequency is inversely proportional to the initial bubble size. Compared with the low flow rate case (Figure 2), the energy content is spread over a wider frequency range, indi-

cating that the bubbly plume contains bubbles with a larger range of sizes, which results from of violent interactions between bubbles.

To examine the influence of the hydrophone locations on the measured acoustic emissions, measurements were taken at a depth of 2.5m and various horizontal distances from the centre of the plume. PSD plots of these measurements are shown in Figure 6 and spectrograms of measurements taken at 0.5m, 1m, and 2m from the plume are illustrated in Figures 7 - 9. Peaks in the PSD plots can be seen up to 3000 Hz for all measurement locations. The spectrograms of data measured at 1m and 2m from the plume show high amplitude peaks occurring consistently at a number for frequencies below 1000Hz. This is in contrast to data measured at 0.5m where constant frequency lines in the spectrogram are less clear. It can be seen that more identifiable lines are present at frequencies below 700 Hz for the higher flow rate case compared with the low flow rate case shown in Figure 3. Improved visualisation in subsequent studies will be used to gain a better understanding of the effect of flow rate on bubble generation.

It should be noted that the contribution of the reverberant field on the bubble measurements could not be easily defined for the high flow rate condition. In addition, further work is required to quantify the transition from the near field region to the far field for a bubbly plume. The data recorded at a depth of 2.5m and a distance of 2.0m away from the plume was judged to best show the peaks that would be related to the formation of large bubbles and thus was used for the bubble size distribution calculation. These experimental results highlight the importance of hydrophone location on the estimation of bubble generation rate from acoustic measurements.
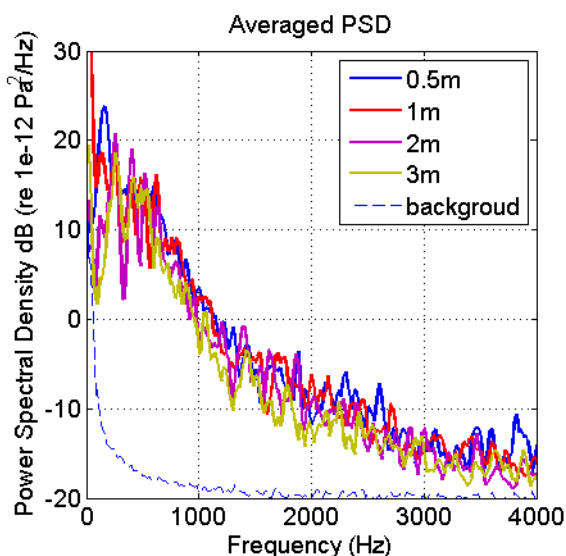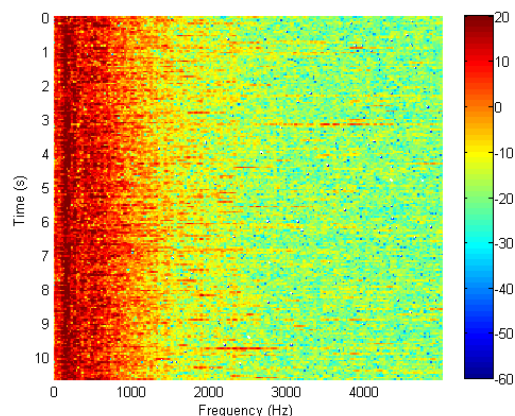

Figure 7. Spectrogram (dB re 10^{-12} Pa^2/Hz) of bubble noise for 8mm orifice measured at d=2.5 m and y=0.5m away from bubbly plume.
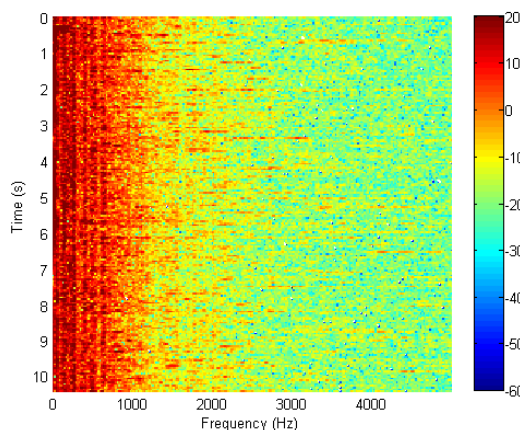

Figure 8. Spectrogram (dB re 10^{-12} Pa^2/Hz) of bubble noise for 8mm orifice measured at d=2.5m and y=1m away from bubbles.
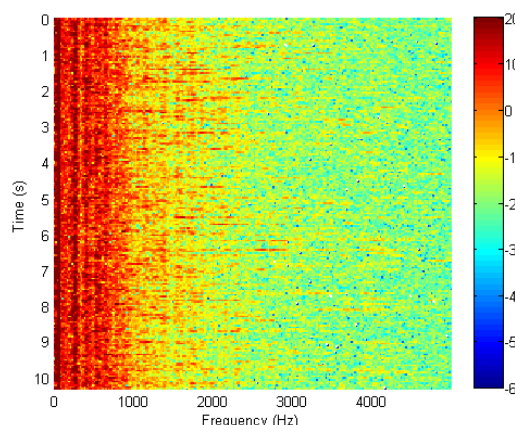

Figure 9. Spectrogram (dB re 10^{-12} Pa^2/Hz) of bubble noise for 8mm orifice measured at d=2.5m and y=2m.

Figure 6. PSD of bubble noise for 8mm orifice measured at d=2.5m and various horizontal distances away from the plume

Bubble generation rate spectrum

The bubble population spectrum is estimated by the model described in equations (2) – (8). In this model, $R_{0\varepsilon i}/R_0$ has to be specified, however, there are few reported data to support a particular value for this parameter. Leighton & Walton (1987) estimated $R_{0\varepsilon i}/R_0 \approx 1\times10^{-5}$ for bubbles smaller than 1mm in radius. Leighton and White (2011) suggested

3.74×10^{-4} for bubbles between 1 and 5 mm in radius. The limited available data show an order of magnitude difference in the value of $R_{0\varepsilon i}/R_0$, for a given bubble radius. In principle, the value should decrease with increasing bubble size. Given the lack of consistent data for the size of bubbles observed in this experiment, different values were used to demonstrate its effect on the bubble generation spectrum. The estimated bubble generation rate spectrum calculated using $R_{0\varepsilon i}/R_0 = 1.5 \times 10^{-6}$, acoustic data measured at $d = 2$m and $y = 1$m, and a flow rate of 8.3×10^{-3} l/s is shown in Figure 10. This position was used because it was believed to best represent the acoustic emission of the bubbly plume as discussed earlier. The flow rate estimated by integrating the number of bubbles is equal to 5.8869×10^{-3} l/s. This gives an error of about 29% compared with the measured flow rate of 8.3×10^{-3} l/s. Increasing the value of $R_{0\varepsilon i}/R_0$ from 1.5×10^{-6} to 1×10^{-5} (as suggested by Leighton and Walton, 1987) produces a similar bubble generation rate spectrum (cf. Figures 10 and 11), but yields a total flow rate of 2.36×10^{-4} l/s, which is significantly lower than the measured value of 8.3×10^{-3} l/s. These findings suggest that the number of bubbles formed is strongly dependent on the magnitude of $R_{0\varepsilon i}/R_0$, but this parameter has negligible influence on the bubble number spectrum. At this flow rate, the bubbly plume is made up of bubbles of radius less than 4mm. Peaks in the bubble generation rate spectrum indicate a few discrete classes of bubbles of a radius smaller than 3mm with a high generation rate. This will be verified by optical measurements in our ongoing study.
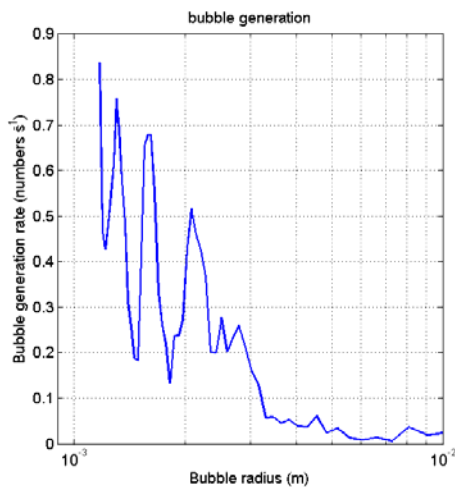

Figure 10. Estimated bubble generation rate spectrum for 8mm orifice based on an acoustic measurement at d=2m and y=1m with $R_{0\varepsilon i}/R_0 = 1.5 \times 10^{-6}$

For the high flow rate condition, the estimated bubble generation rate spectrum calculated using $R_{0\varepsilon i}/R_0 = 1.5 \times 10^{-6}$ is given in Figure 12. With the increase in flow rate, the bubbly plume is predicted to have a significant number of large bubbles with radii between 1 and 8 mm. The bubble generation rate has also increased significantly. Calculations were also performed with the parameter of $R_{0\varepsilon i}/R_0$ increased to 1.0×10^{-5}. The calculated flow rates were 1.0253×10^{-1} l/s and 2.36×10^{-3} l/s for $R_{0\varepsilon i}/R_0 = 1.5 \times 10^{-6}$ and $R_{0\varepsilon i}/R_0 = 1.0 \times 10^{-5}$ respectively. Both values significantly under-estimated the measured flow rate of 3.33×10^{-1} l/s. The large discrepancy between the estimated and measured total flow rates found

for the high flow rate case may be partially attributed to errors in the flow rate measurement. A more accurate measurement procedure will be implemented in future to help resolve the discrepancy.
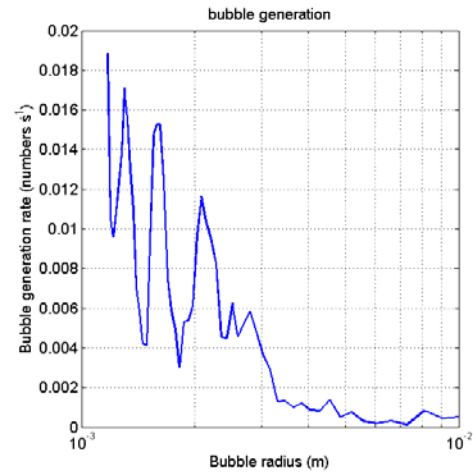

Figure 11. Estimated bubble generation rate spectrum for 8mm orifice based on an acoustic measurement at d=2m and y=1m with $R_{0\varepsilon i}/R_0 = 1 \times 10^{-5}$.

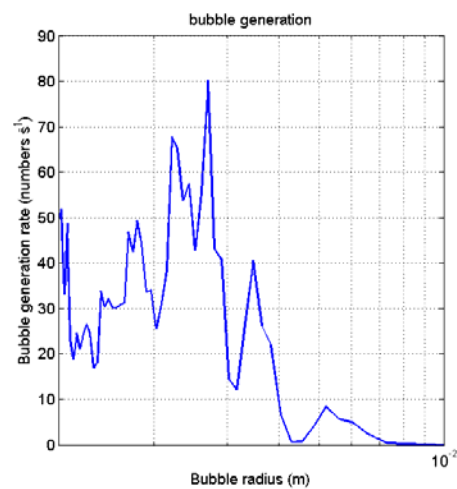**Figure 12.** Estimated bubble generation rate spectrum for 8mm orifice based on an acoustic measurement at d=2.5m and y=2.0m with $R_{0\varepsilon i}/R_0 = 1.5 \times 10^{-6}$.

The underestimation of bubble generation rates was not expected, particularly when using a value of $R_{0\varepsilon i}/R_0 = 1.5 \times 10^{-6}$ as this is lower than that suggested by Leighton & Walton (1987). In addition, the raw acoustic signal may have been increased by reverberation in the tank and this would lead to an over-estimation of the bubble generation rate. The better agreement between measured and predicted flow rates for the low flow rate case (8.3×10^{-3} l/s) is consistent with the finding of Deane and Stokes (2008) that the ratio $R_{0\varepsilon i}/R_0$ decreases with an increase in bubble radius. Leighton and White (2011) applied this model to different situations with $R_{0\varepsilon i}/R_0 = 3.74 \times 10^{-4}$ and reported an error of about 11%. It is thus reasonable to conclude that the governing mechanism of the initial condition $R_{0\varepsilon i}/R_0$ is complex and requires further research.

CONCLUSION

The acoustic emissions from a bubble plume have been measured. The bubble generation rates have been estimated using the measured acoustic emission, and they are strongly dependent on the initial displacement of the bubbles. For the conditions studied, it appears that the ratio of the initial displacement of a bubble to its initial radius should be smaller than the values suggested by the limited available data. However, despite the discrepancy between estimated and measured total flow rate, it can be concluded from the current model that for the same orifice size, increasing flow rate produces more large bubbles and leads to stronger acoustic emission.

It should be noted that the estimated bubble generation rate spectrum will change slightly depending on where the acoustic emission data is measured. It has been found that the hydrophone data measured at a closer location to the orifice predicts a higher generation rate for larger bubbles, which is expected. Incorporation of multiple hydrophones in an array, coupled with more accurate flow measurement should lead to a more accurate estimation of the bubble generation spectrum.

REFERENCES

Blake, W 1986, *Mechanics of Flow-Induced Noise*, Academic Press

Chen, L Li, Y & Manasseh, R 1998, 'Numerical study of bubble coalescence', *Proc. 3rd International Conference on Multiphase Flow*, Lyon, France, June, paper No. 626.

Chen, L Garimella, SV Reizes, JA & Leonardi, E 1999, 'The development of a bubble rising in a viscous liquid', *J. Fluid Mech.*, Vol. 387, pp.61-96.

Chen, L & Manasseh, R 2001, 'Air Release from an Underwater Opening', *4th International Conference on Multiphase Flows*, New Orleans, USA, July, paper No. 348.

Deane, GB & Stokes, MD 2008, 'The acoustic excitation of air bubbles fragmenting in sheared flow', *J. Acoust. Soc. Am.,* Vol 102, pp. 2671-2689.

Gavigan, JJ, Watson, EE & King III, WF, 1974, 'Noise generation by gas jets in a turbulent wake', *J. Acoustic Soc. Am.* Vol. 56, No.4 pp1094-1099.

Leighton, TG & Walton, AJ 1987, 'An experimental study of the sound emitted from gas bubbles in a liquid', *Eur. J. Phys.* Vol8, pp. 98-104.

Leighton, TG & White, PR 2011, 'Quantification of undersea gas leaks from carbon capture and storage facilities, from pipelines and from methane seeps, by their acoustic emissions', *Proc. R. Soc. A*, doi:10.1098/rspa.2011.0221.

Leighton, TG 1994, *Acoustic Bubble*, Academic Press.

Longuet-Higgins, M 1990, "Bubble noise spectra". *J. Acoust. Soc. Am.*, Vol 87(2), 652-661 (1990).

Minnaert, M 1933, 'On musical air bubbles and the sound of running water, Phil. Mag.,Vol 16, pp. 235-248.

Sevik, M & Park, SH 1972, 'The splitting of drops and bubbles by turbulent fluid flow', *J. Basic Eng. Trans.* ASME, Paper No. 72-WA/FE-32, pp. 1-8.

Strasberg, M 1956, 'Gas bubbles as sources of sound in liquids', *J. Acoust. Soc. Am.*, Vol 28, pp.20-26.